Neuron
Article

Locomotor Rhythm Generation Linked to the Output of Spinal Shox2 Excitatory Interneurons

Kimberly J. Dougherty,[1,6] Laskaro Zagoraiou,[2,3,6,*] Daisuke Satoh,[4,5] Ismini Rozani,[3] Staceyann Doobar,[2] Silvia Arber,[4,5] Thomas M. Jessell,[2] and Ole Kiehn[1,*]
[1]Mammalian Locomotor Laboratory, Department of Neuroscience, Karolinska Institutet, 171 77 Stockholm, Sweden
[2]Howard Hughes Medical Institute, Kavli Institute for Brain Science, Departments of Neuroscience and Biochemistry and Molecular Biophysics, Columbia University, New York, NY 10032, USA
[3]Biomedical Research Foundation of the Academy of Athens, 115 27 Athens, Greece
[4]Biozentrum, Department of Cell Biology, University of Basel, 4056 Basel, Switzerland
[5]Friedrich Miescher Institute for Biomedical Research, 4058 Basel, Switzerland
[6]The authors contributed equally to this paper
*Correspondence: lzagoraiou@bioacademy.gr (L.Z.), ole.kiehn@ki.se (O.K.)
http://dx.doi.org/10.1016/j.neuron.2013.08.015

SUMMARY

Locomotion is controlled by spinal networks that generate rhythm and coordinate left-right and flexor-extensor patterning. Defined populations of spinal interneurons have been linked to patterning circuits; however, neurons comprising the rhythm-generating kernel have remained elusive. Here, we identify an ipsilaterally projecting excitatory interneuron population, marked by the expression of Shox2 that overlaps partially with V2a interneurons. Optogenetic silencing or blocking synaptic output of Shox2 interneurons (INs) in transgenic mice perturbed rhythm without an effect on pattern generation, whereas ablation of the Shox2 IN subset coinciding with the V2a population was without effect. Most Shox2 INs are rhythmically active during locomotion and analysis of synaptic connectivity showed that Shox2 INs contact other Shox2 INs, commissural neurons, and motor neurons, with preference for flexor motor neurons. Our findings focus attention on a subset of Shox2 INs that appear to participate in the rhythm-generating kernel for spinal locomotion.

INTRODUCTION

Locomotion is a complex motor behavior that involves the patterned activation of limb and body muscles. In vertebrates, the rhythmic muscle activities that drive locomotion depend on the activity of spinal neural networks termed central pattern generators (CPGs). At their core, CPGs comprise interconnected groups of excitatory and inhibitory neurons, the output of which is sufficient to generate aspects of both motor rhythm and pattern. In brief, rhythm-generating neurons impose locomotor timing and set the pace of the rhythm. Patterning neurons direct the sequential activation of motor neuron pools. Thus, coordinated motor pattern adheres to the timing set by the rhythm generator. From work on the CPGs for swimming in lamprey and *Xenopus* tadpole, ipsilaterally projecting excitatory interneurons (iEINs) are thought to be responsible both for rhythm generation and the activation of motor neurons, whereas inhibitory commissural interneurons are involved in left-right alternation (Buchanan and Grillner, 1987; Roberts et al., 1998; Li et al., 2006). Similarly for the mammalian CPG that directs walking, ipsilateral inhibitory neurons are involved in setting up flexor-extensor alternation and contralaterally-projecting commissural neurons ensure left-right coordination (Talpalar et al., 2011; Butt et al., 2002a; Butt and Kiehn, 2003; Zhong et al., 2006; Jankowska, 2008; Kiehn, 2006). Mammalian rhythm-generating interneurons are thought to be excitatory (Kiehn, 2006; Grillner and Jessell, 2009) and to project ipsilaterally (Kiehn, 2006), but their molecular and functional identity has remained elusive.

The classification of spinal neurons on the basis of embryonic expression of transcription factors has permitted identification of excitatory and inhibitory interneuron populations (Jessell, 2000; Goulding, 2009). Two classes of glutamatergic iEINs have been analyzed: V2a and Hb9 interneurons. V2a interneurons express Chx10, comprise the major set of iEINs in the ventral spinal cord (Al-Mosawie et al., 2007; Lundfald et al., 2007) and exhibit rhythmic activity during locomotion (Dougherty and Kiehn, 2010a; Zhong et al., 2010). Embryonic ablation of V2a neurons leads to the disruption of normal left-right alternation in a speed-dependent manner, and the inability to evoke locomotion by stimulation of descending fibers (Crone et al., 2008, 2009), but does not impact the rhythmogenic capacity of the spinal CPG. Yet in zebrafish spinal cord, interneurons analogous to mammalian V2a neurons have been implicated in rhythm generation (McLean et al., 2008; Eklöf-Ljunggren et al., 2012). iEINs marked by the expression of the transcription factor Hb9 are rhythmically active but, by virtue of Hb9 expression in motor neurons, their influence on rhythmic motor output remains unclear (Hinckley and Ziskind-Conhaim, 2006; Wilson et al., 2005). The contribution of other molecularly defined classes of ventral excitatory interneurons to rhythmogenic behaviors is uncertain.

Here, we set out to identify interneuron populations involved in the generation of motor rhythm. We describe a set of iEINs that expresses the homeodomain transcription factor Shox2

(Shox2 INs). The Shox2$^+$ and Chx10$^+$ interneuron subsets exhibit substantial overlap, but ~25% of Shox2 INs lack Chx10 expression, uncovering a previously unappreciated set of spinal iEINs. Blocking the output of Shox2 INs has a marked impact on spinal rhythmogenic activity. Locomotor frequency decreases while left-right and flexor-extensor alternation remains intact, an effect not mimicked by inactivation of Chx10$^+$ V2a interneurons. Electrophysiological and anatomical analysis of Shox2 INs reveals recurrent interconnections, input to motor neurons in a flexor-biased manner, and rhythmic bursting during fictive locomotor activity. These findings imply that Chx10^{off} Shox2$^+$ INs constitute part of the rhythm-generating network, providing key insights into the logic of iEIN diversity and motor rhythmicity.

RESULTS

Shox2 Marks a Subpopulation of Excitatory Interneurons in the Ventral Spinal Cord

To identify distinct populations of iEINs, we performed a microarray screen for genes preferentially enriched in ventral spinal cord at lumbar levels (Zagoraiou et al., 2009; Table S1 available online). We found that the homeobox gene *Shox2* was expressed at P0-P1 by a set of interneurons present along the entire rostrocaudal axis of the spinal cord. In the transverse plane, these neurons occupied an intermediate domain that extended mediolaterally from close to the central canal to the edge of the gray matter (Figure 1A).

To define the origin and distribution of Shox2 neurons in greater detail we generated a *Shox2::Cre* mouse line (Figure 1B) and performed lineage tracing with fluorescent protein (FP) conditional reporter mice (*Rosa26-YFP/tdTomato* and *Z/EG* lines). Comparison of FP and endogenous protein expression revealed that Shox2 expression begins around E11.5 and persists until postnatal stages, although expression is extinguished from many FP$^+$ interneurons at later embryonic stages: ~80% of FP$^+$ neurons expressed Shox2 at E12.5, compared to ~35% at P0-P1 (Figures 1C and 1D). In our subsequent analyses, we define Shox2 interneurons (Shox2 INs) on the basis of *Shox2::Cre* directed FP expression, independent of maintained Shox2 expression. To define the neurotransmitter phenotype of Shox2 INs, we monitored the status of vGluT2 expression in *Shox2::Cre; Tau-GFP-nlsLacZ* mice. We found that > 98% of Shox2$^+$ neurons expressed *vGluT2* transcript (n = 3; Figure 1E), indicating that Shox2 INs are glutamatergic.

We next addressed the extent of subtype diversity of Shox2 INs. The settling position of Shox2 INs overlapped that of V2a neurons, marked by expression of the transcription factor Chx10 (Jessell, 2000; Crone et al., 2008; Lundfald et al., 2007). We therefore determined the extent of overlap of FP and Chx10 expression in lumbar spinal cord tissue derived from *Shox2::Cre*; *FP* reporter mice (Figure 1F). At P0-1, we found that 77% of Shox2 INs coexpressed Chx10 and conversely that 60% of Chx10$^+$ INs were marked by Shox2-directed FP expression (Figure 1F). These studies reveal three distinct populations of ventrally positioned vGluT2$^+$ excitatory interneurons: Shox2^{only} INs, Chx10^{only} INs, and Shox2/Chx10^{double} INs.

We next addressed the origin and diversity of the Shox2 IN class of EINs. Since Chx10$^+$ INs derive from the p2 progenitor domain we considered whether Shox2^{only} INs are p2 domain derived. p2 domain progenitors give rise to inhibitory GATA3-derived V2b and V2c INs as well as to excitatory Lhx3$^+$/Chx10$^+$ V2a INs (Peng et al., 2007; Panayi et al., 2010). But our analysis of FP-marked neurons in *Shox2::Cre; ROSA26-YFP* reporter mice at E13.5 revealed that Lhx3$^+$, FP$^+$, Chx10^{off} INs (Figure 1G) comprised ~10% of the total Shox2 IN population, indicating that some Chx10^{off} Shox2 INs are distinct from inhibitory V2b and V2c neurons, and likely derive from p2 domain progenitors. In addition, at E13.5 we detected a dorsally positioned set of FP$^+$, Lhx3^{off} Shox2 INs that expressed Lbx1 or Isl1 (Figures 1H–1J), presumably dorsal di4-6 and di3 domain derivatives (Helms and Johnson, 2003; Müller et al., 2002). FP$^+$ Lbx1$^+$ Shox2 INs represented 6% and FP$^+$ Isl1$^+$ INs 12% of the total Shox2 IN population. We also detected Lmx1b expression within a dorsolateral Shox2 IN subpopulation (Figure S1), indicating that the Lbx1$^+$ and Isl1$^+$ subsets of Shox2 INs fall within the dI5 and dI3 populations, respectively.

This analysis reveals that Shox2 INs comprise four molecularly distinct subsets: two ventrally derived populations defined by Chx10$^{on/off}$ status and two minor dorsally derived populations defined by Lbx1 or Isl1 expression. We term the p2-derived Chx10^{off} class of Shox2 INs V2d INs, to distinguish them from Chx10^{on} V2a neurons.

The Axons of Shox2 INs Project Ipsilaterally

To reveal the extent of dendritic arbors and the laterality of axonal projections of Shox2 INs, we biocytin-filled identified GFP labeled neurons in *Shox2cre; Z/EG* spinal cords. The dendritic trees of Shox2 INs were sparse with processes that extended in the mediolateral plane (Figures 1K and 1L). None of 28 biocytin-filled Shox2 INs gave rise to axons that projected contralaterally (Figures 1K and 1L). We also tested whether Shox2 INs could be back-labeled by tetramethylrhodamine dextran (TMR) applied contralaterally in a parasagittal slit cut along the ventral surface of the lumbar spinal cord (L1–L6). By this criterion, fewer than 1% of GFP-expressing neurons had axons crossing the midline (Figure 1M). Thus, Shox2 INs innervate ipsilateral targets.

Ablation of Shox2$^+$ V2a Neurons Has Modest Effects on Locomotor-like Activity

Elimination of Chx10 INs in mice disrupts left-right alternation at high speeds of locomotor activity in vitro and in vivo and decreases the fidelity of locomotor burst amplitude and duration in vitro (Crone et al., 2008, 2009). To examine whether Shox2$^+$ V2a INs contribute to these motor behavioral phenotypes, we analyzed locomotor-like activity in *Shox2::Cre; Chx10-Inl-DTA* mice in which DTA expression had been targeted selectively to Shox2$^+$ V2a INs. In *Shox2::Cre; Chx10-Inl-DTA; Z/EG* mice we detected a 98% reduction in the incidence of Shox2$^+$ V2a INs, along with an 81% reduction in the total number of Shox2 INs (Figures 2B and 2C).

Exposure of spinal cords isolated from neonatal *Shox2::Cre; Chx10-Inl-DTA* mice (*Shox2-Chx10DTA*) to 5-hydroxytryptamine (5-HT) and N-methyl-D-aspartate (NMDA) induced a stable locomotor-like activity resembling that seen in control preparations (Figure 2A). Application of NMDA increased the locomotor frequencies in a concentration-dependent manner but revealed

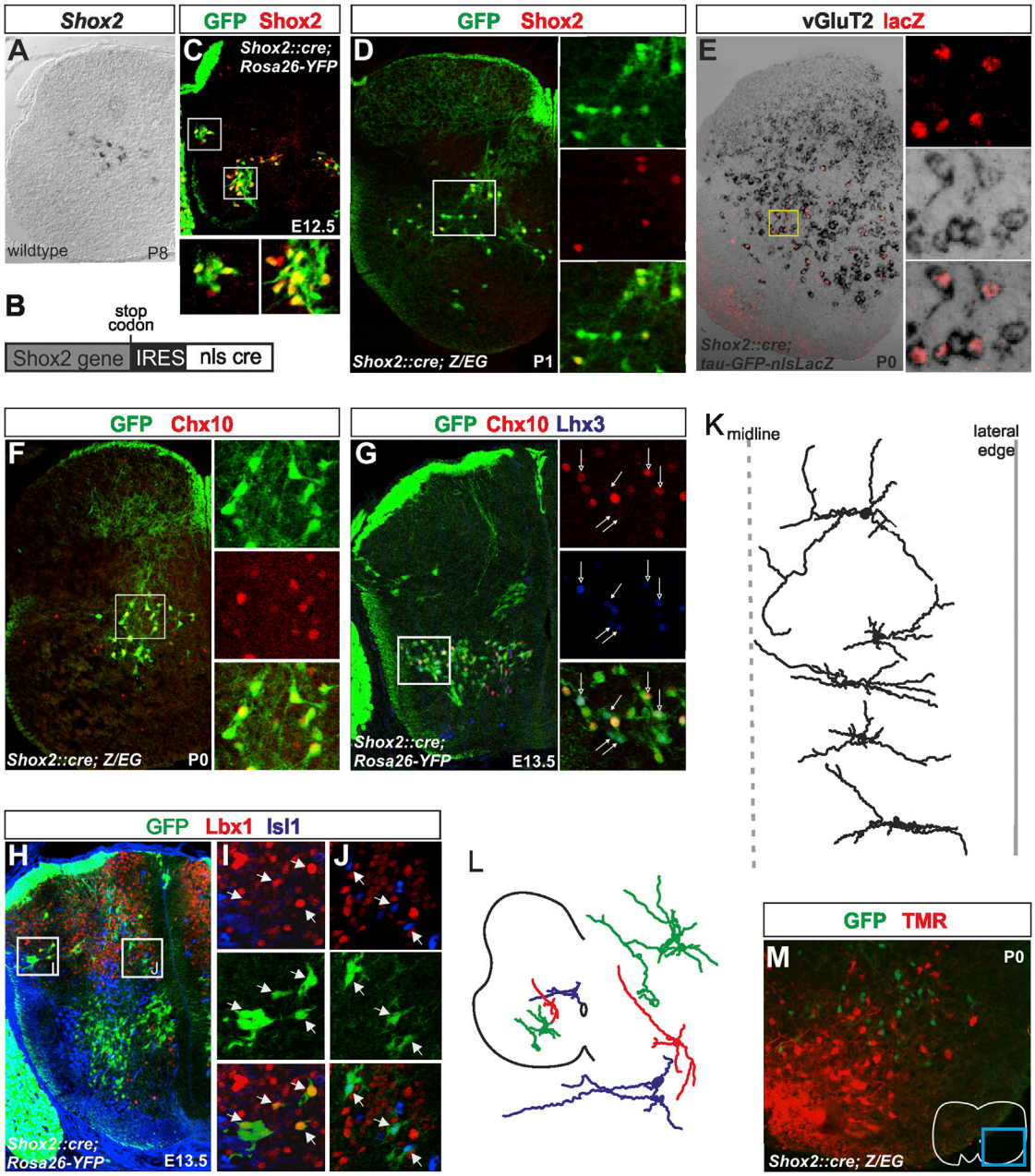

Figure 1. Shox2 Defines a Subpopulation of Glutamatergic Neurons in the Ventral Spinal Cord that Projects Ipsilaterally

(A) In situ hybridization for *Shox2* in a mouse lumbar hemicord at P8.

(B) Shox2-IRES-nls-Cre construct used for the *Shox2::Cre* mouse.

(C) GFP expression in *Shox2::Cre; Rosa26-YFP* mouse at E12.5. Shox2 antibody labeling (red) showing 80% ± 2% (n = 12, N = 3) overlap with GFP (green). Note the dorsal population of Shox2 seen embryonically (left box).

(D) Shox2 is downregulated postnatally. Distribution and overlap of Shox2 antibody labeling (red) and GFP (green) is shown in *Shox2::Cre; Z/EG* mouse at P1. In *Shox2::Cre; Z/EG* (n = 26, N = 3) and *Shox2::Cre; Rosa26-YFP* (n = 24, N = 3) mice at P0–1, Shox2 protein is found in 35% ± 1% of FP^+ neurons.

(E) Combined in situ hybridization/immunohistochemistry showing *vGluT2* transcript detection in Shox2-Cre^+ neurons. Nearly all $Shox2^+$ neurons (99% ± 0.5%, n = 3) are $vGluT2^+$.

(F) Chx10 antibody labeling (red) compared to Shox2 (GFP) expression at P0. At this age, 77% ± 2% (n = 65, N = 7) of Shox2 INs express $Chx10^+$. Conversely, 40% of $Chx10^+$ INs are Shox2 INs.

(G) Shox2 INs from the p2 domain can be divided into two groups: $Shox2^+$ V2a neurons that express Shox2, Chx10, and Lhx3 (open arrows), and $Shox2^+$ V2d neurons that are $Shox2^+$ and $Lhx3^+$, but $Chx10^-$ (closed arrows); 74% ± 1% and 8% ± 1% (n = 30, N = 2) of Shox2 INs are V2a and V2d, respectively.

(H–J) $Shox2^+$ non-V2 neurons are located more dorsally embryonically. Small subsets of Lbx1 (red) and Isl1 (blue) neurons at E13.5 are Shox2 INs (H). Most Shox2 INs located dorsolaterally are $Lbx1^+$ (I). $Lbx1^+$ neurons comprise 12% ± 2% (n = 17, N = 2) of the Shox2 INs, although Shox2 INs are only a minor

(legend continued on next page)

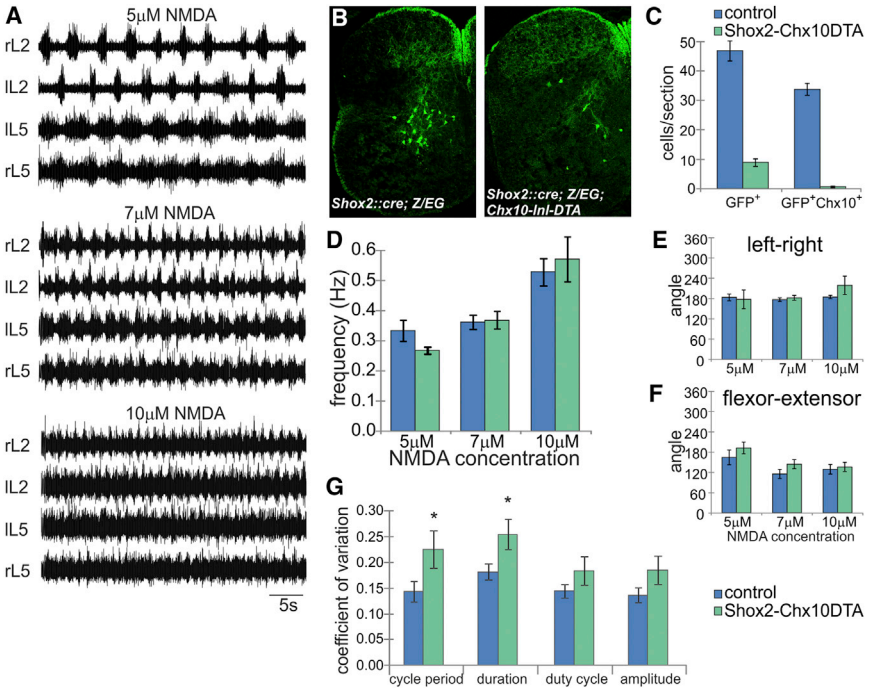

Figure 2. Ablation of Shox2⁺ V2a Neurons Does Not Affect Locomotor Frequency or Change the Left-Right/Flexor-Extensor Coordination

(A) Locomotor-like activity induced by 8 μM 5-HT with 5 μM, 7 μM, or 10 μM NMDA in a *Shox2cre; Chx10lnlDTA* isolated spinal cord.

(B) Lumbar hemisections from *Shox2::cre; Z/EG* and *Shox2::cre; Chx10lnlDTA; Z/EG* mice at P0 show a reduction in the number of Shox2 INs by 79% (n = 46, N = 6).

(C) Quantification of the number of GFP neurons and double-positive GFP⁺Chx10⁺ neurons (± SEM) in control (blue) and Shox2-Chx10DTA (green) mice. The number of Shox2 INs (GFP⁺) is decreased by 81% in Shox2-DTA mice and Shox2⁺ V2a neurons (GFP⁺Chx10⁺) are decreased by 98%.

(D) Mean locomotor frequency (± SEM) in Shox2-Chx10DTA mice (green: 0.27 ± 0.01 Hz at 5 μM, 0.37 ± 0.03 Hz at 7 μM, 0.57 ± 0.08 Hz at 10 μM; n = 6, 13, and 6, respectively) is not significantly different than littermate matched controls (blue: 0.33 ± 0.03 Hz at 5 μM, 0.36 ± 0.02 Hz at 7 μM, 0.53 ± 0.05 Hz at 10 μM; n = 9, 14, and 11, respectively).

(E and F) The phase angles between left-right L2 roots (E) and ipsilateral L2-L5 (flexor-extensor, F) are not significantly different between control (blue) and Shox2-Chx10DTA (green) mice at any frequency of locomotion. Error bars represent ± SEM.

(G) There is a greater variation in cycle period and burst duration in Shox2-Chx10DTA mice compared to controls. Error bars represent ± SEM.

no difference in burst frequencies between control and *Shox2-Chx10DTA* mice (Figure 2D). We detected pronounced left-right and flexor-extensor alternation at all locomotor burst frequencies examined, with a preferred vector at ~180° in isolated spinal cords from both control and *Shox2-Chx10DTA* mice (Figures 2E and 2F). The coefficients of variation for the main locomotor parameters (cycle period, burst duration, and amplitude) were increased in *Shox2-Chx10DTA* mice as compared to controls (Figure 2G) similar to locomotor changes after elimination of all V2a neurons (Crone et al., 2008, 2009). However, cycle period, burst duration, and burst amplitude were not significantly different between controls and *Shox2-Chx10DTA* mice. These findings argue that Shox2⁺ V2a INs are not responsible for changes in left-right patterning in V2a IN-depleted mice (Crone et al., 2008, 2009), but do contribute to increased motor burst variability.

Eliminating the Output of Shox2 INs Reduces the Frequency of Locomotor-like Activity

To evaluate the contribution of the entire population of Shox2 INs to locomotor output, we used a conditional genetic approach to delete *vGluT2* expression from these neurons, thus blocking vesicular glutamate accumulation, and consequently evoked transmitter release (see Talpalar et al., 2011). *Shox2::Cre* mice were crossed with a conditional floxed *vGluT2* allele, to produce offspring with a selective loss of *vGluT2* (see Experimental Procedures) from this set of excitatory INs, as revealed by loss of transcript expression from > 85% of Shox2 INs in *Shox2::Cre; vGluT2$^{fl/\Delta}$; Tau-GFP-nlsLacZ* mice (Figure S2).

We first evaluated the impact of loss of Shox2 IN output in *Shox2::Cre; vGluT2$^{fl/\Delta}$* mice (*Shox2-vGluT2$^{\Delta/\Delta}$*) on locomotor frequency. Locomotor-like activity was evoked with combination of NMDA and 5-HT applied directly to the isolated spinal cord with varying concentrations of NMDA (5–10 μM), while keeping the concentration of 5-HT (8 μM) constant (Figures 3A and 3B). As there were no differences seen between mice lacking one copy of *vGluT2*, mice without Cre expression, and wild-type mice, all littermates that were not *Shox2-vGluT2$^{\Delta/\Delta}$* were grouped together as controls. In controls, the mean locomotor frequencies increased with increasing NMDA concentrations (Figures 3A and 3C). The frequencies of locomotor activity in

population of Lbx1⁺ INs. J. Many of the dorsomedial Shox2 INs are Isl1⁺; 6% ± 0.5% (n = 17, N = 2) of Shox2 INs are Isl1⁺ and Shox2 INs are a small fraction of Isl1⁺ INs.

(K) Examples of reconstructed cells filled intracellularly in dorsal-horn-removed preparations. Cells were from different preparations. Midline (dashed line) and lateral edge (solid line) show the relative mediolateral positioning of the Shox2 INs and their processes.

(L) Reconstructions of three Shox2 INs filled intracellularly in transverse sections. Relative positions of the cells are shown in the schematic. Colors in the schematic correspond to the colors of the cells shown in higher magnification.

(M) Contralaterally located back-labeled neurons do not express Shox2. Inset shows the location of the figure. The slit in the drawing indicates the location of TMR application. *Shox2::Cre; ZEG* endogenous fluorescence is seen in green, TMR back-labeled neurons are red. Four of 407 GFP⁺ (n = 20; N = 2) were retrogradely labeled with TMR.

See also Figure S1.

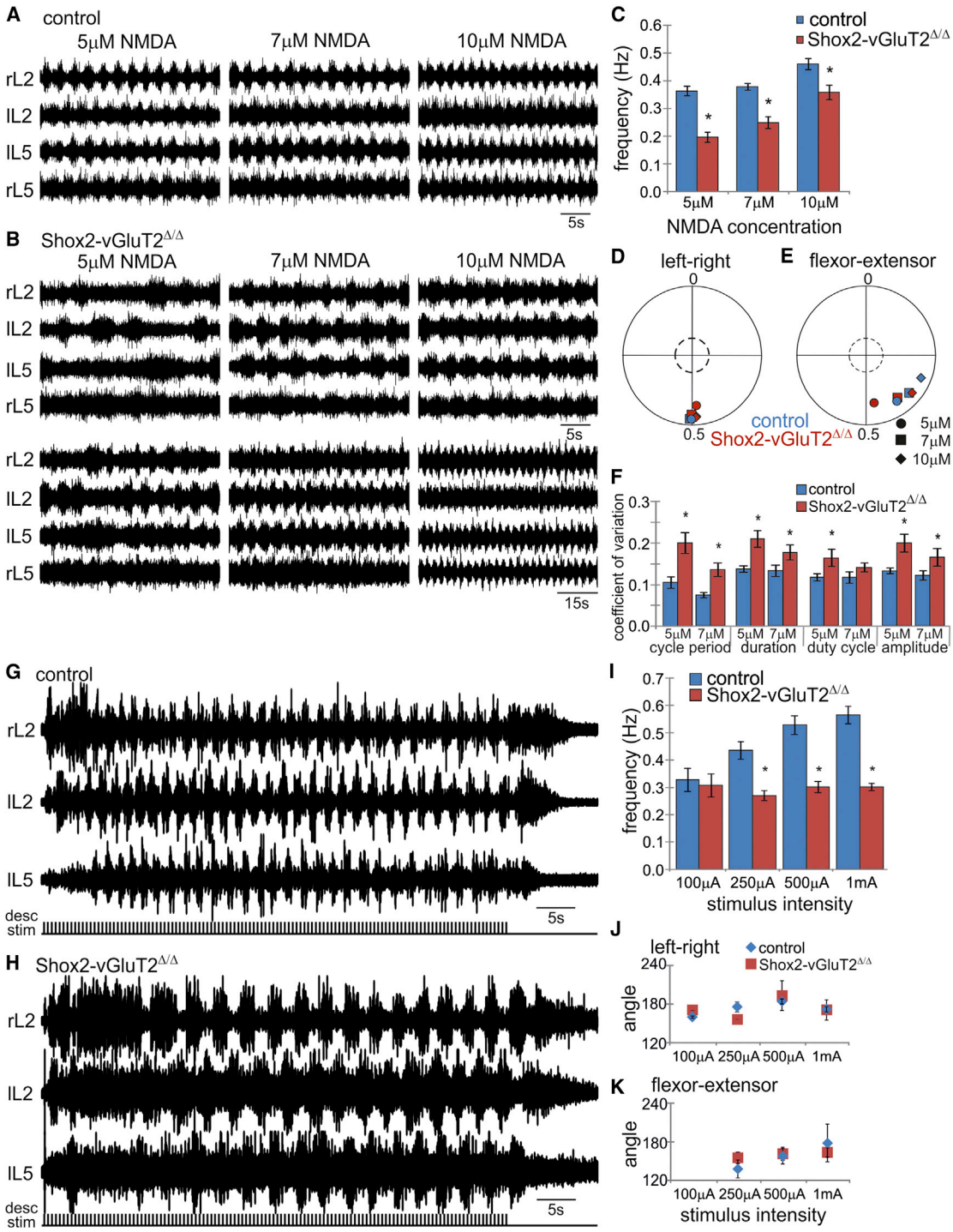

Figure 3. Elimination of vGluT2 from Shox2 INs Leads to Reduced Frequency of Drug-Evoked and Neural-Evoked Locomotor-Like Activity but no Change in Coordination

(A) Drug evoked locomotor-like activity in a control spinal cord at three concentrations of NMDA. All include 8 μM 5-HT.

(B) Drug evoked locomotor-like activity in a *Shox2-vGluT2*$^{\Delta/\Delta}$ spinal cord at the same four concentrations of NMDA as in (A). All include 8 μM 5-HT. Note that the time scale of the top section matches that seen in (A). The bottom section is from the same files as the top section but on a compressed time scale to illustrate the coordination.

(C) Frequency of both control and *Shox2-vGluT2*$^{\Delta/\Delta}$ locomotor-like activity increases with increasing NMDA concentration (control (n = 17): 0.36 ± 0.02 Hz at 5 μM, 0.38 ± 0.01 Hz at 7 μM, 0.46 ± 0.02 Hz at 10 μM). However, the frequency of *Shox2-vGluT2*$^{\Delta/\Delta}$ cords (n = 11) is always lower (0.20 ± 0.02 Hz at 5 μM, 0.25 ±± 0.02 Hz at 7 μM, 0.36 ± 0.03 Hz at 10 μM). Error bars represent ± SEM. * indicates $p < 0.005$.

(legend continued on next page)

the *Shox2-vGluT2*$^{\Delta/\Delta}$ cords also increased with increasing NMDA concentration but were significantly lower than in controls (Figure 3C). Frequency is determined by burst duration, interburst interval, and the variability of bursts. The locomotor burst duration was increased in *Shox2-Vglut2*$^{\Delta/\Delta}$ cords compared to controls, while the duty cycle was unchanged, indicating a corresponding increase in the interburst interval in *Shox2-vGluT2*$^{\Delta/\Delta}$ cords compared to controls. The coefficients of variation for the main locomotor parameters (cycle period, burst duration, amplitude, and duty cycle) were increased in *Shox2-vGluT2*$^{\Delta/\Delta}$ cords as compared to controls (Figure 3F). Thus, silencing or ablating an iEIN population results in a lower locomotor frequency and suggests that Shox2 INs play a rhythm-generating role in locomotion.

We next evaluated left-right (IL2-rL2) and flexor-extensor (L2–L5) coordination. For all frequencies, there was a significant left-right and flexor-extensor alternation (preferred direction around 0.5 in the circular plots; Figures 3D and 3E). The increased variability in burst parameters (see above) likely contributes to the slightly weaker left-right coupling in *Shox2-vGluT2*$^{\Delta/\Delta}$ cords (seen as shorter r-vectors at lower frequencies of locomotion Figures 3D and 3E). At higher speeds of locomotion, the variability decreased but coupling was unaltered. Flexor-extensor coupling was not significantly different at any locomotor frequency.

These findings underscore a role for Chx10^{off} Shox2 INs in rhythm generation (a change in frequency) but with little to no effect on left-right and flexor-extensor coordination. However, in addition to influencing locomotor frequency, elimination of Shox2 INs also affected the stability of the rhythm, in a manner similar to that seen when all V2a neurons were ablated (Crone et al., 2008), and when the Shox2^{+} V2a neurons are eliminated (this study). The reduction in locomotor frequency is seen in *Shox2-vGluT2*$^{\Delta/\Delta}$ mice, where both Shox2^{+} V2a INs and Shox2^{+} non-V2a INs are silenced, but not in *Shox2-Chx10DTA* mice, where Shox2^{+} V2a INs alone are ablated, suggesting a specific role for Shox2^{+} non-V2a INs in rhythm generation.

Shox2-vGluT2$^{\Delta/\Delta}$ Mice Show Similar Phenotypes in Drug- and Neural-Evoked Locomotion

Bath application of locomotor drugs exposes all spinal neurons to neural excitants uniformly and tonically, which likely is not the case in vivo. To test the locomotor phenotype of *Shox2-vGluT2*$^{\Delta/\Delta}$ mice in a more physiological context, we evaluated locomotor-like activity induced by brainstem stimulation, an efficient way of evoking bouts of locomotor activity. Rhythmic ventral root bursting was elicited by descending fiber stimulation in both control and *Shox2-vGluT2*$^{\Delta/\Delta}$ spinal cords (Figures 3G and 3H). In controls, burst frequency increased with stimulus strength (Figure 3I). However, locomotor frequency in *Shox2-vGluT2*$^{\Delta/\Delta}$ cords was slower than controls at all stimulus intensities, apart from the lowest (Figure 3I). Additionally, in *Shox2-vGluT2*$^{\Delta/\Delta}$ spinal cords locomotor frequency failed to increase with increasing stimulus intensity (Figure 3I). Left-right and flexor-extensor activities were in alternation (offset ~180°) in both control and *Shox2-vGluT2*$^{\Delta/\Delta}$ mice at all stimulation intensities tested (Figures 3J and 3K). These experiments show that Shox2 INs may be involved in mediating the descending locomotor drive and/or generating the rhythmic activity in the spinal cord.

Although some of the reduction in frequency seen in neural-evoked locomotion may be due to a loss of Shox2-related descending drive, the drug-induced method to evoke locomotor-like activity bypasses the neural-evoked pathways for initiating locomotor-like activity. Together, the lower drug-evoked and stimulus-evoked locomotor frequencies seen in *Shox2-vGluT2*$^{\Delta/\Delta}$ cords as compared to controls suggest that spinal Shox2 INs play a significant role in rhythm generation.

Optogenetic Inactivation of Shox2 INs Phenocopies Chronic Silencing of Shox2 INs

To probe whether chronic blockade of neuronal output induces reactive changes in network organization, we attempted to inactivate Shox2 INs acutely, through light activation of halorhodopsin expressed in Shox2 INs. We found that *Shox2::Cre*; *Rosa26-eNphR-YFP* (Madisen et al., 2012) mice expressed enhanced halorhodopsin (eNpHR) channels in Shox2 INs. Intracellular recordings from identified Shox2 INs revealed that light pulses hyperpolarized Shox2 INs by 8–15 mV (n = 4; Figure 4A).

To evaluate the effect of acute inactivation of Shox2 INs, locomotion was induced with 7 μM NMDA and 8 μM 5-HT in the isolated spinal cord of *Shox2::Cre*; *Rosa26-eNphR-YFP* mice and 30 s light pulses were delivered to the ventral side of the spinal cord. Locomotor frequency before exposure to light (mean = 0.36 ± 0.02 Hz) was similar to that seen in

(D and E) Circular plots showing left-right (D) and flexor-extensor (E) phasing in controls and *Shox2-vGluT2*$^{\Delta/\Delta}$ mice in different concentrations of NMDA. The dotted inner circles represent significance at p = 0.05. Left and right alternation is observed in all conditions as seen by values clustered around 0.5. Flexor-extensor bursts are also alternating in all conditions.

(F) Coefficients of variation at the two lowest NMDA concentrations. There is a pronounced increase in the variability in several locomotor parameters in *Shox2-vGlut2*$^{\Delta/\Delta}$ at the lowest NMDA (5 μM) concentration as compared to control and this variability is lessened with increased NMDA concentrations. Error bars represent ± SEM. * indicates $p < 0.05$.

(G and H) Locomotion induced by stimulation of descending fibers in control (G) and *Shox2-vGluT2*$^{\Delta/\Delta}$ (H) spinal cords. The bottom traces (desc stim) indicate the stimulus pulses.

(I) Frequency of the descending fiber evoked locomotor-like activity increases with stimulation intensity in controls (blue: 0.33 Hz at 100 μA [n = 8/18], 0.44 Hz at 250 μA [n = 16/18], 0.53 Hz at 500 μA [n = 18/18], and 0.56 Hz at 1 mA [n = 18/18]) but remains constant in *Shox2-vGluT2*$^{\Delta/\Delta}$ mice (red: 0.31 Hz [n = 2/10], 0.27 Hz [n = 10/10], 0.30 Hz [n = 10/10], and 0.30 Hz [n = 9/10] at 100, 250, 500, and 1 mA, respectively). Error bars represent ± SEM. * indicates $p < 0.001$.

(J) The left-right phasing is not affected in the *Shox2-vGluT2*$^{\Delta/\Delta}$ (red) as compared to the controls (blue) mice. Data are shown as mean ± SEM.

(K) The flexor-extensor phasing is not affected in the *Shox2-vGluT2*$^{\Delta/\Delta}$ (red) as compared to control (blue) mice. Data are shown as mean ± SEM.

See also Figure S2.

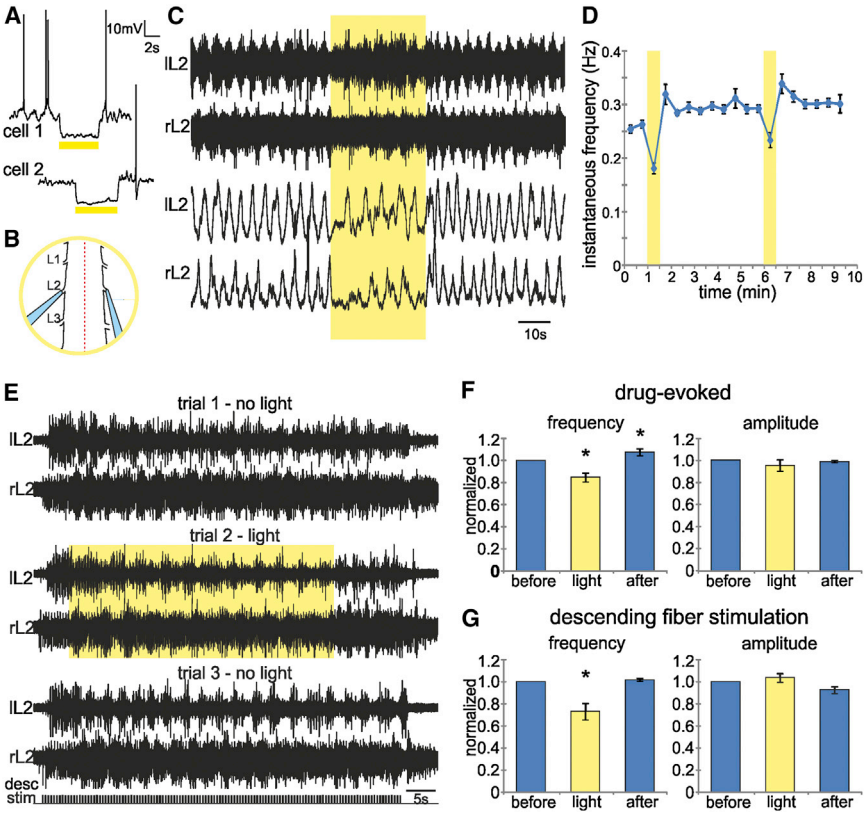

Figure 4. Optogenetic Silencing of Shox2 INs Phenocopies the Chronic Silencing

(A) Two examples of light-induced hyperpolarization in Shox2 cells. Yellow bars indicate the duration and timing of the light stimulus.

(B) Cartoon showing the approximate area of the cord that was illuminated during locomotion experiments.

(C) Locomotor-like activity induced by 7 μM NMDA and 8 μM 5-HT in a *Shox2::Cre; RC-eNpHR* cord. Top two traces are raw ventral root recordings and the bottom two traces are recordings that have been rectified and smoothed. Area shaded yellow indicates when the yellow light was turned on to activate the halorhodopsin, thereby inactivating Shox2 INs.

(D) Mean instantaneous frequency calculated in 30 s bins. The yellow shaded area indicates when the yellow light was on for 30 s. The recordings in (A) are from the same file (from approximately time 0–2.5 min).

(E) Locomotor-like activity evoked by descending fiber stimulation in a *Shox2::Cre; RC-eNpHR* cord. The same stimulation protocol was run in three successive trials, spaced apart by ~4 min. During trial 2, the yellow light was turned on for 45 s (yellow shaded region). Stimulation pulses (desc stim) are shown in bottom trace.

(F) Mean frequency and amplitude during drug-induced locomotor-like activity (n = 7) before, during, and after light pulse. Error bars represent ± SEM.

(G) Mean frequency and burst amplitude during the light pulse for trial 2 and for the same corresponding time in trials 1 and 3 (n = 6). All data are mean ± SEM.

controls (0.38 ± 0.01 Hz, p = 0.43). However, exposure of the rostral lumbar cord to light (Figure 4B) decreased the locomotor frequency to a maintained lower frequency (85% ± 4% of control) for the duration of illumination (Figures 4C, 4D, and 4F). After light extinction, locomotor frequency returned to prestimulus values after an initial poststimulus rebound (108% ± 3% of control; see Warp et al., 2012). The effects of photoillumination on burst amplitude were variable. In some spinal cords (n = 4), amplitude was reduced at the start of the light pulse and gradually increased in amplitude throughout the stimulation (as in Figure 4C). In others (n = 3), there was no obvious effect of the light-stimulus on burst amplitude. Left-right and flexor-extensor coordination were not affected by the change in locomotor frequency in any of the experiments.

When locomotor-like activity was induced by electrical stimulation of descending fibers, light inactivation of Shox2 INs during neural-evoked locomotor-like activity decreased locomotor frequency to 73% ± 7% of control values, but had no consistent effect on the amplitude of locomotor bursts (Figures 4E and 4G). Together, these experiments demonstrate that acute inactivation of the entire population of Shox2 INs has effects on the frequency of locomotor-like activity similar to those seen when the entire population of Shox2 INs was chronically removed from the network.

Most Shox2 INs Are Rhythmically Active during Locomotor-like Activity

Neurons involved in locomotor rhythm generation should be rhythmically active during locomotion. We tested the activity of GFP-labeled neurons in the *Shox2::Cre; Z/EG* mice during locomotor-like activity using dorsal-horn-removed preparations in which Shox2 INs were visually identified for whole-cell recordings, while monitoring motor output from ventral roots (Figure 5A). Locomotor-like activity was induced by application of 5-HT and NMDA. Of 70 Shox2 INs analyzed during locomotor-like activity, 52 fired action potentials while the other 18 remained subthreshold. We found that 62% of spiking neurons (32/52) fired rhythmically in relation to the local ventral root (Figures 5B, 5D, and 5E), while 69% (36/52) exhibited clear phase-related membrane potential oscillations. Of the nonspiking neurons, 61% (11/18) exhibited membrane potential oscillations in phase with ventral root bursts (Figures 5C and 5F). Thus, Shox2 INs are rhythmically active during drug-evoked locomotor-like activity.

We next analyzed, separately, the set of Shox2 INs located in predominantly flexor-related (L2 and L3) or extensor-related (L4 and L5) segments. We found that 20/27 of the Shox2 INs in L2/L3 spiked rhythmically whereas only 12/25 of the L4/L5 Shox2 INs spiked rhythmically. For both rhythmic firing and membrane oscillations, there was a clear flexor dominance. We found that 70% of neurons in L2/L3 (14/20) spiked in phase

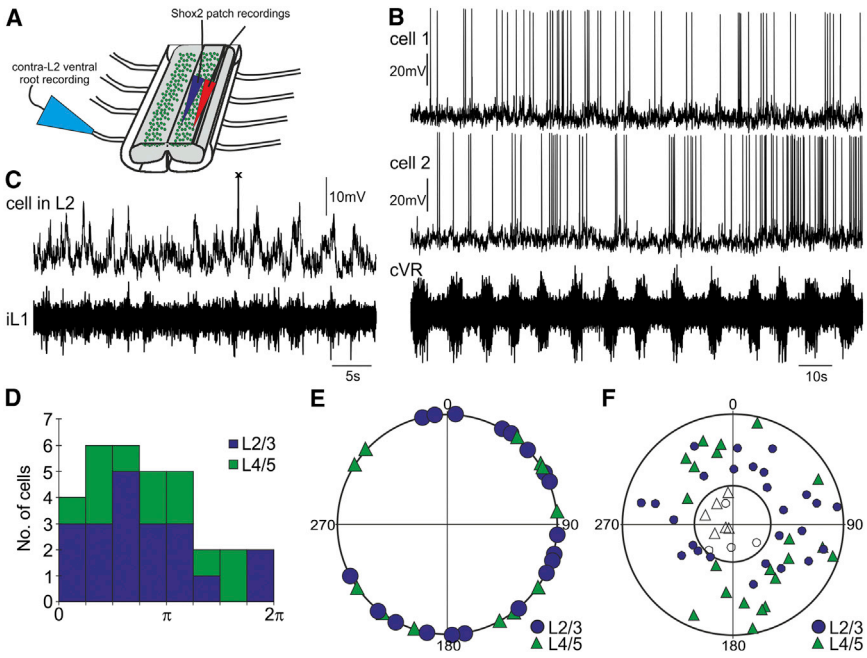

Figure 5. Most Shox2 INs Are Rhythmically Active during Locomotor-Like Activity

(A) Cartoon showing simultaneous recordings from two Shox2 INs and a contralateral ventral root (cVR) in a dorsal-horn-removed preparation.

(B) Recordings from two rhythmic Shox2 INs and the contralateral ventral root (cVR), as depicted in (A).

(C) An example of Shox2 IN membrane potential oscillations during locomotor-like activity as seen in the ipsilateral ventral root (iVR). The x is a single spike that was cut off for scaling of the oscillations.

(D and E) Preferred firing phase of all rhythmically spiking Shox2 INs displayed in a histogram (D) and a circular plot (E). Neurons located in segments L2–L3 are depicted in purple and those located in segments L4–L5 are depicted in green. All cells are plotted relative to the root that is ipsilateral to the recorded cell and located in the same segment.

(F) Phasing of membrane potential oscillations of Shox2 INs located in L2–L3 (purple) and in L4–L5 (green). The inner circle is the significance level of $p = 0.05$. Points falling inside the inner circle are not significant and those outside the inner circle are cells with rhythmic oscillations that show significant phasing relative to the local ventral root.

with local flexor-related ventral root activity, whereas in L4/L5, spiking was equally divided into flexor- and extensor-related neurons. Approximately 60% of L2/L3 (15/26) and of L4/L5 (13/21) Shox2 INs had the depolarizing peak in the flexor phase. Therefore, regardless of segment, most Shox2 INs are rhythmically active in the flexor-phase. This finding is in contrast to rhythmic Chx10-GFP neurons (a mix of Shox2^{+} and Shox2^{off} V2a neurons), where flexor- and extensor-related neurons were evenly distributed throughout the lumbar cord (Dougherty and Kiehn, 2010a, 2010b).

Premotor Shox2 INs Exhibit Flexor Motor Neuron Biased Connectivity Profiles

Our electrophysiological findings on Shox2 INs reveal preferential activation of Shox2 INs during the flexor phase of locomotion. To determine whether this feature is correlated with connectivity profiles detected at the premotor level, we evaluated connectivity between Shox2 INs and motor neurons. First, we injected a floxed-synaptophysin-GFP adeno-associated virus into the spinal cords of P3 *Shox2::Cre* mice and monitored the presence of GFP-labeled Shox2 IN terminals on motor neurons at P17 (Figures 6A–6D). We observed many Shox2 IN terminals in lamina IX, often in apposition to motor neuron somata and proximal dendrites (Figures 6A–6C). Shox2 IN terminals were also detected in the intermediate zone and in lamina VIII, the settling position of other CPG interneurons. High-resolution reconstructions of synaptic input from Shox2 INs to motor neurons innervating ankle flexor tibialis anterior (TA) or ankle extensor gastrocnemius (GS) muscles, specifically marked by retrograde labeling from the muscle, revealed a Shox2 IN synaptic bias toward flexor (TA) motor neurons (Figure 6D).

To determine the position of Shox2 INs that are monosynaptically connected to motor neurons, we performed retrograde transsynaptic labeling by the application of rabies viruses with monosynaptic restriction (Stepien et al., 2010; Tripodi et al., 2011). We carried out unilateral virus injections coincidently into several hindlimb muscles to target many premotor neurons. We found that ~50% of Shox2 INs in the rostral lumbar spinal cord were transsynaptically marked from hindlimb innervating motor neurons, whereas this fraction decreases caudally (Figures 6E–6G). Contour plots of premotor and nonpremotor Shox2 INs show that within the entire cohort of Shox2 INs, premotor Shox2 INs are biased toward a more lateral compartment in the spinal cord than nonpremotor Shox2 INs, defining two distinct peaks in the overall Shox2 IN distribution (Figure 6H).

Our results show a segregation in location of Shox2 neurons based on their connectivity or lack of connectivity to motor neurons (Figure 6H). Therefore, we next determined if the Shox2 INs connecting with flexor and extensor motor neurons are also segregated anatomically. In experiments tracing monosynaptic rabies virus spread separately from GS and TA motor neurons, we found that the percentage of Shox2 INs labeled from TA was three-fold greater than from GS (Figures 6I–6L). Whereas Shox2 INs constituted 5% of last order neurons labeled from the TA motor neurons, they only made up 1.5% of GS premotor neurons (Figure 6L), confirming the clear flexor bias of these connections observed also by anterograde tracing (Figures 6D and 6L). This flexor dominance was evident at the level of all Shox2 premotor INs, regardless of rostral-caudal location. Both GS and TA injections labeled Shox2 INs in overlapping areas of the most lateral area of lamina VII (Figures 6I–6K) demonstrating that the Shox2 INs projecting to flexor and extensor motor neurons are intermingled.

In summary, our findings suggest that Shox2 INs segregate into a laterally located premotor population and a more

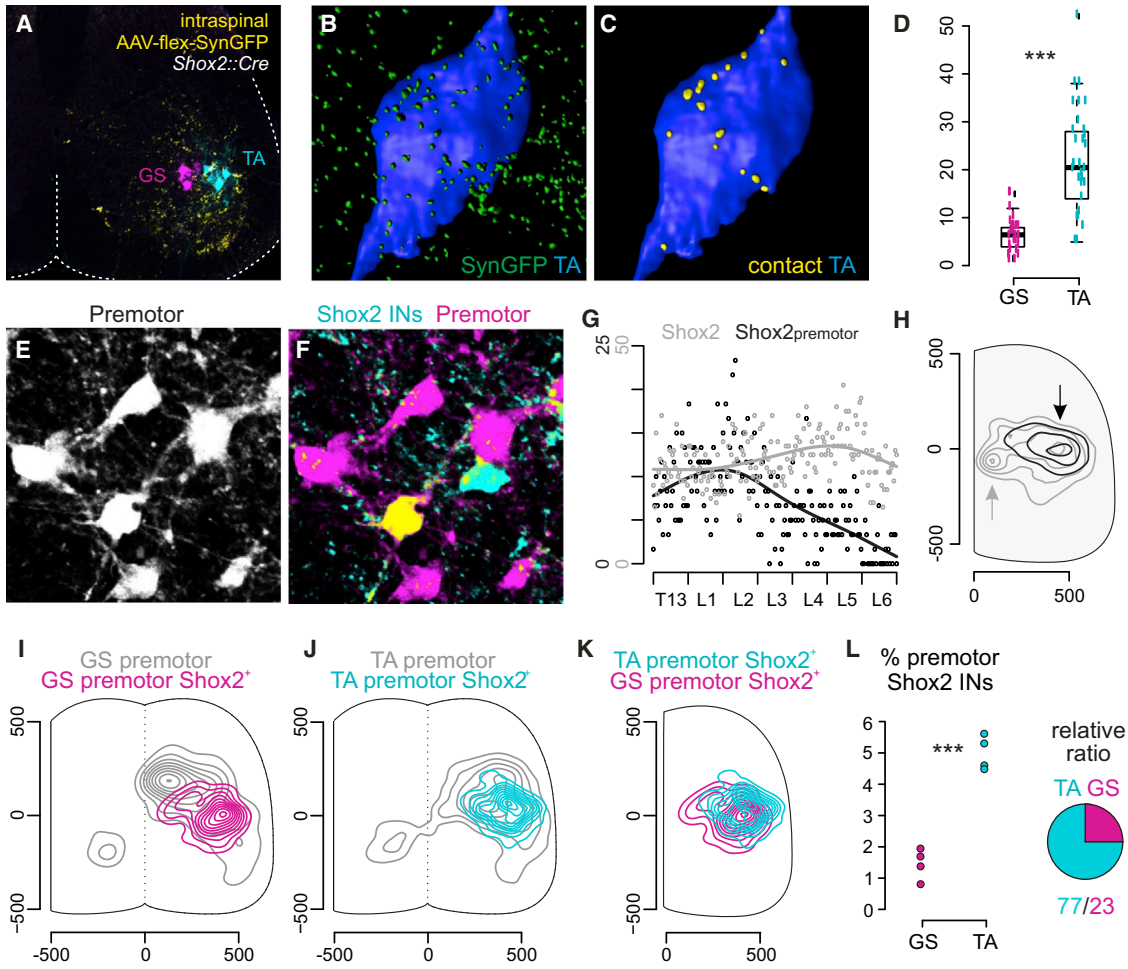

Figure 6. A Subset of Shox2 INs Preferentially Contacts Flexor Motor Neurons

(A–D) Anatomical evidence that Shox2 INs contact motor neurons. Section of lumbar spinal cord from a *Shox2::Cre* mouse after spinal injection of AAV-flex-SynaptophysinGFP virus (A). All Shox2 terminals seen around a single TA motor neuron (B). Shox2$^+$ contacts on a TA motor neuron (C). Quantification of Shox2 terminals in close apposition to gastrocnemius (GS; n = 30 neurons) and tibialis anterior (TA; n = 28 neurons) motor neurons (D).

(E–H) Shox2 INs with direct connections to motor neurons were labeled by transsynaptic monosynaptically restricted rabies virus injected into most muscles in one hindlimb. (E) Premotor neurons labeled by the virus injection. (F) Same panel as in (E) with premotor virus-labeled neurons in purple and Shox 2 neurons in *Shox2::Cre; Rosa26-tdTomato* mice in cyan. A double-labeled premotor Shox2 IN is shown in yellow. (G) Plot of rostral-caudal distribution of Shox2 INs (gray) and Shox2 INs with direct connections to ipsilateral motor neurons (black) in the lumbar spinal cord (L1–L6; note different scales on y axis). (H) Contour plots depicting mediolateral location of Shox2 INs with direct connections to motor neurons (black) relative to the entire Shox2 IN population (gray).

(I–L) Shox2 INs connect preferentially to TA motor neurons in comparison to GS motor neurons. Contour plots of the location of neurons labeled by monosynaptically restricted transsynaptic rabies virus injected into the extensor gastrocnemius (GS) muscle are shown in (I); all GS premotor neurons are shown in gray, whereas Shox2 premotor INs are shown in purple. Contour plots of the location of neurons labeled by monosynaptically restricted transsynaptic rabies virus injected into the TA muscle are shown in (J); all TA premotor neurons are shown in gray, whereas Shox2 premotor INs are shown in cyan. An overlay of the contour plots for flexor- and extensor-related Shox2 premotor INs is shown in (K). (L) The percentage of TA and GS premotor neurons that are Shox2 INs and the relative ratio of TA to GS Shox2 premotor INs (p value < 0.0001; n = 4 independent experiments each).

medially-positioned population, which corresponds to the location of the Shox2$^+$ nonpremotor INs. Additionally, within the premotor Shox2 IN population, there is a connectivity bias toward flexor motor neurons.

Connectivity Pattern of Shox2 INs in the Lumbar Spinal Cord

Based on findings in other locomotor networks, rhythm-generating neurons are interconnected and provide excitation to several other identifiable CPG neurons. We therefore further evaluated the connectivity of Shox2 INs (Figure 7A).

Shox2 INs Form Interconnections

Rhythm-generating neural networks in *Xenopus* tadpole and lamprey are thought to be excitatory neurons that are recurrently, although sparsely, interconnected (Roberts et al., 1998; Grillner, 2003). To probe recurrent connectivity within the Shox2 population, we performed dual recordings from fluorescently labeled Shox2 INs in *Shox2::Cre; Z/EG* mice in

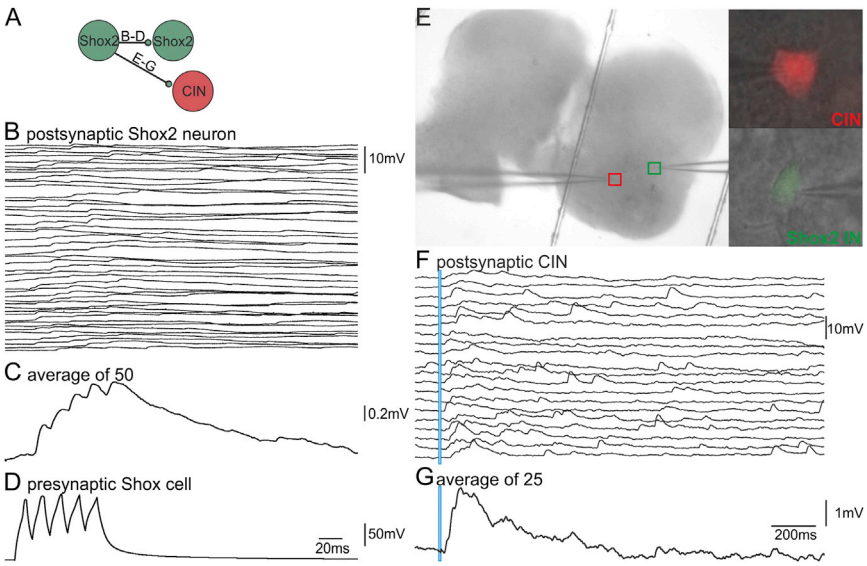

Figure 7. Neural Connectivity of Shox2 INs

(A) Schematic of connections shown in the rest of the figure. Letters correspond to the relevant figure panels.

(B–D) A subset of Shox2 INs makes excitatory connections to other Shox2 INs. Five suprathreshold current pulses were delivered to the presynaptic Shox2 IN while averaging the response in the postsynaptic neuron (B). The compound EPSP from an average of 50 trials is seen in (C).

(E–G) Subsets of Shox2 INs make synaptic connections to commissural interneurons (CIN). Location of Shox2 IN and CIN in *Shox2::Cre; Z/EG mouse* (E). Red box shows the backfilled CIN. Green box shows the Shox2 IN. A 10 ms puff of kainate (blue box) delivered to the somata of the Shox2 IN elicits an EPSP in the CIN, as seen in single trials (F) and in an average of 25 sweeps (G). See also Figure S3.

dorsal-horn-removed preparations. Depolarizing synaptic connections were detected in 4 of 41 pairs of Shox2 INs (Figures 7B–7D). In all four cases, coupled pairs were found in close proximity and connections were unidirectional: spiking in one neuron resulted in EPSPs in the second neuron, but there was no reciprocal activation. In two of the connected pairs, EPSPs built up with each successive spike (Figure 7C). The amplitude of the EPSPs ranged from 0.05 to 1 mV. Thus, Shox2 INs are sparsely interconnected, without direct monosynaptic feedback. Connectivity among neurons in excitatory populations may be expected and has been examined in a similar manner in other populations (Dougherty and Kiehn, 2010a; Zhong et al., 2010; Wilson et al., 2005; Hinckley and Ziskind-Conhaim, 2006), although electrical connectivity has been demonstrated (Hinckley and Ziskind-Conhaim, 2006; Zhong et al., 2010). Here, we show glutamatergic synaptic connections that likely underestimate the number of connections that exist.

A Subset of Shox2 INs Makes Synaptic Connections to Commissural Neurons

We next examined whether Shox2 INs provide direct excitation to commissural interneurons (CINs). CINs serve an essential role in coordinating motor activity on the left and right sides the body (Grillner, 2006; Kiehn, 2006). CINs are rhythmically active during locomotion in rodents (Butt et al., 2002b; Butt and Kiehn, 2003; Quinlan and Kiehn, 2007) and may be driven by excitatory neuronal activity during locomotion (Butt et al., 2002a). We therefore looked for connections between Shox2 INs and identified CINs in a transverse spinal slice preparation (Figure 7E). CINs were recorded in whole-cell mode while spikes were elicited in Shox2 INs by application of short (10 ms) kainate (100 mM) puffs delivered from a microelectrode placed in juxtaposition to individual Shox2 INs (Jonas et al., 1998; Figure S3), permitting stimulation of up to four Shox2 INs, in turn, for each recorded CIN. Of 26 recorded CINs, four received short latency EPSPs (mean amplitude: 1.5 mV) in response to kainate applications to a Shox2 IN (Figures 7F and 7G). Thus, a subset of Shox2 INs projects directly to commissural neurons located in the same segments.

In summary, the electrophysiological connectivity studies demonstrate connections between Shox2 INs and neurons projecting ipsilaterally and contralaterally in the ventral spinal cord.

DISCUSSION

Studies of spinal networks have long implicated excitatory interneurons in the generation of locomotor rhythm, but their identity and precise contribution to CPG circuitry has remained ambiguous. This study of mouse locomotor networks reveals that a subset of lumbar spinal iEINs defined by expression of the homeodomain transcription factor Shox2, in the absence of Chx10, has a role in rhythm generation. Our findings provide insight into the molecular identity of iEINs involved in mammalian locomotor control.

Shox2 Expression Defines a Discrete Class of Ventral Excitatory Interneurons

The homeodomain protein Shox2 marks a discrete subset of ventrally positioned glutamatergic neurons with ipsilateral axons and targets. In postnatal spinal cord, we find that ~75% of all Shox2 INs coexpress Chx10 and thus derive largely or exclusively from the p2 progenitor domain (Ericson et al., 1997). Previous studies have shown that p2 domain progenitors give rise to excitatory V2a (Chx10$^+$; Ericson et al., 1997; Peng et al., 2007), and inhibitory V2b/c (Gata3$^+$/Sox1$^+$; Panayi et al., 2010) neurons. Our study defines an additional p2-derived excitatory IN set, termed V2d INs and thus subdivides p2-derived excitatory INs into two populations that differ in the status of Shox2 expression. A small contingent of Shox2 INs represents excitatory neurons belonging to the Isl1$^+$ dI3 and Lbx1$^+$ dI5 populations. Recognition of the molecular diversity of Shox2 INs (*V2a* and non-*V2a*) and V2a neurons (*Shox2*$^+$ and *Shox2*^{off}) has provided genetic entry points to test the functional role of Shox2 INs in locomotion.

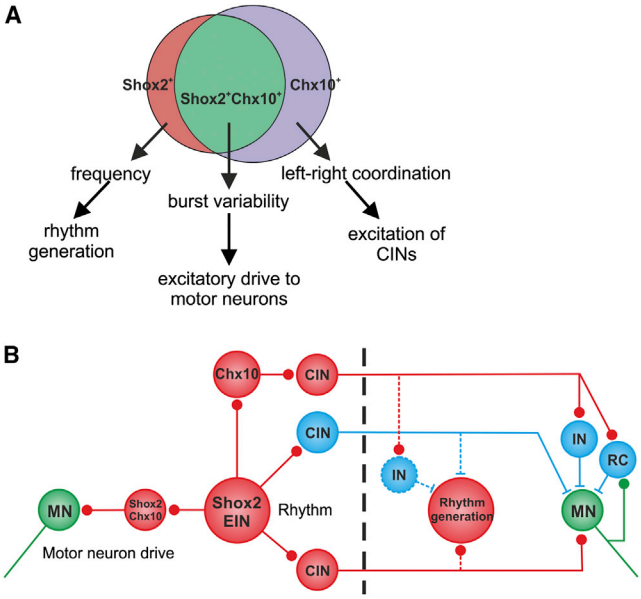

Figure 8. Conceptual Model of Shox2 INs in the Hindlimb Locomotor Network

(A) Summary chart of the different roles of Shox2^{+} V2a, Shox2^{+} non-V2a, and Shox2^{off} V2a neurons.

(B) Network diagram depicting the suggested position of the Shox2^{+} V2a, Shox2^{+} non-V2a, and Shox2^{off} V2a neurons with relationship to left-right circuits and motor neurons. Shox2^{+} non-V2a neurons, along with other yet to be identified excitatory interneurons (EINs), make up a rhythm-generating kernel. These Shox2^{+} non-V2a neurons likely provide rhythmic drive to other ipsilaterally and contralaterally (CIN) projecting locomotor-related neurons. Shox2^{+} V2a neurons are downstream from the rhythm-generating kernel and direct excitation to ipsilateral motor neurons (MNs). Shox2^{off} V2a neurons project to commissural neurons (CIN) as determined in previous work (Crone et al., 2008).

Ablation of Shox2^{+} V2a Neurons Has Modest Effects on Locomotor-like Activity

Ablation of all V2a INs (Crone et al., 2008, 2009), results in a disruption in left-right alternation, accompanied by an increased variability of locomotor burst amplitude and duration (Crone et al., 2008, 2009). Since we have established a division in V2a neurons based on the expression of Shox2 (Shox2^{+} V2a and Shox2^{off} V2a), we have explored the functions associated with these two populations by specifically ablating Shox2^{+} V2a INs in *Shox2::Cre; Chx10-Inl-DTA* mice. These mice displayed an enhanced degree of variability in burst amplitude and periodicity, without an impact on the frequency of the rhythm or left-right and flexor-extensor activity. The increased variability of motor output in the absence of major rhythm and pattern disruptions suggests a decreased fidelity of excitatory input direct to motor neurons. By subtraction, we attribute the disrupted left-right alternation seen when all V2a neurons are ablated (Crone et al., 2008, 2009) to Shox2^{off} V2a interneurons (Figure 8A). Together, these data suggest that the Shox2^{+} V2a neurons are involved in stabilizing burst amplitude and locomotor frequency while the Shox2^{off} V2a neurons drive the excitation of commissural pathways involved in left-right motor coordination.

Shox2^{+} Non-V2a Neurons Are Involved in Rhythm Generation but Not Patterning

Shox2^{+} V2a INs are the majority of Shox2 INs, but there is a significant population of Shox2^{+} non-V2a neurons that is left unaffected in the Shox2-Chx10DTA experiments. The most pronounced effect of silencing the output of all Shox2 INs was a reduction in the frequency of locomotion. This reduction in rhythm frequency was accompanied by increases in amplitude and burst variability of the locomotor activity but a retained flexor-extensor and left-right alternation, as compared to control mice. The increased amplitude variability and burst variability of the locomotor activity was similar to that seen both in V2a-ablated (Crone et al., 2008, 2009) and Shox2-Chx10DTA mice, and therefore may be ascribed to ablation of the population that is commonly affected in all circumstances, the Shox2^{+} V2a neurons (see above and Figure 8A). On the other hand, the reduction in frequency is, by exclusion, selective to the ablation of Shox2^{+} non-V2a neurons.

The Shox2^{+} non-V2a neurons were not found previously as studies focusing on rhythm generating neurons had concentrated on ventral progenitors. Many Shox2^{+} non-V2a neurons originate dorsally and the ventral Shox2^{+} non-V2a population (V2d) had not been previously described. One of the Shox2^{+} non-V2a populations, or a combination of them, is likely to be involved in rhythm generation. Of the Shox2^{+} non-V2a subpopulations, it is unlikely to be the Shox2^{+} dI3 INs since use of Isl1-Vglut2$^{\Delta/\Delta}$ mice to silence glutamatergic transmission in the entire dI3 population does not affect locomotor rhythm (Bui et al., 2013; Bui et al., 2012, Soc. Neurosci., abstract). Therefore, the Shox2^{+} dI5 INs and/or the V2d neurons are likely responsible for decreased locomotor frequency seen in this study.

Another hallmark of vertebrate excitatory rhythm generating neurons is their recurrent connectivity (Li et al., 2006; Parker and Grillner, 2000). Although connectivity was seen among Shox2 INs, it was sparse and we cannot ascribe this connectivity directly to Shox2^{+} non-V2a INs. It is notable that synaptic connectivity was not observed in previous studies of V2a neurons in the rodent spinal cord in Chx10-GFP mice (Dougherty and Kiehn, 2010a; Zhong et al., 2010), nor has it been seen among excitatory Hb9 neurons (Wilson et al., 2005; Hinckley and Ziskind-Conhaim, 2006).

The rostrocaudal distribution of rhythmicity found in Shox2 INs may match with the subsets of Shox2 INs having a role in rhythm generation. Thus, the rhythm generating capability in the spinal cord is distributed (Kiehn and Kjaerulff, 1998) throughout the lumbar cord but with a rostral (L1–L3) dominance (Cazalets, 2005; Kiehn and Kjaerulff, 1998). Notably, this rostral-caudal difference in rhythmicity was not seen in V2a neurons, as Chx10-GFP rhythmic neurons were equally distributed along the lumbar spinal cord (Dougherty and Kiehn, 2010a, 2010b; Zhong et al., 2010).

Could there be an alternate explanation for the decrease in frequency observed in this study? Shox2 neurons could provide drive to the rhythm generating neurons—in which case a reduction in the glutamatergic drive to rhythm generating neurons would account for the decrease in locomotor frequency. We do not favor this possibility, since the majority of Shox2 neurons,

particularly in more rostral segments, are rhythmically active during locomotion, thereby placing them either as part of the rhythm generator or downstream from it. If Shox2 neurons provide tonic drive to rhythm generating neurons, they would have to be located locally as Shox2-halorhodopisin experiments involved application of yellow light to an area of approximately three lumbar segments—with a consequent reduction in locomotor frequency.

Another possibility is that the non-V2a Shox2 neurons are not rhythm generating but the effect seen is due to a nonspecific decrease in the number of excitatory neurons required for rhythm generation. Essentially when a critical mass of excitatory cells is eliminated, the frequency will drop. However, the Chx10 neurons outnumber the Shox2 neurons by at least 20%–25%. Therefore, if the critical excitatory cell mass hypothesis was correct, we would expect there to be a pronounced reduction in frequency in Chx10DTA experiments (that Crone et al., 2008 did not see), an intermediate reduction in the Shox2-Chx10DTA experiments (that we did not see), and a reduction in the frequency in Isl1-vGlut2$^{\Delta/\Delta}$ experiments (which Bui et al., 2012, Soc. Neurosci., abstract did not see). Available evidence therefore does not fit this hypothesis.

Our findings implicate an excitatory neural population in the generation of rhythmicity. We note that the activity of inhibitory neurons involved in reciprocal inhibition between rhythm-generating centers could also influence the frequency of the motor rhythm. Decreasing inhibition in such populations of inhibitory neurons will phase-delay the switching between half-centers, thereby decreasing the frequency of the locomotor rhythm. This effect is most likely what is observed after ablation of inhibitory En1^{+} neurons (Gosgnach et al., 2006) suggesting that at least part of this population is responsible for reciprocal inhibition between rhythm-generating half-centers.

Connectivity of Shox2 INs Defines Distinct Microcircuits in the Locomotor Network

In addition to connectivity between Shox2 INs, some Shox2 INs provide direct excitation to commissural neurons. Although we show that Shox2^{off} V2a neurons are necessary for normal left-right alternation (see above and Figure 8A), these are not marked by GFP in the *Shox2::Cre; Z/EG*. Therefore, these findings demonstrate that Shox2^{+} V2a and/or Shox2^{+} non-V2a INs also project to commissural pathways. We speculate that Shox2^{+} non-V2a neurons are likely candidates for these projections. So why is left-right coordination not affected in the Shox2–*vGluT2*$^{\Delta/\Delta}$ or Shox2-eNpHR mice? The most likely explanation for this is that the Shox2^{+} non-V2a INs and the Shox2^{off} V2a INs drive commissural pathways active at different speeds of locomotion (Figure 8B; see also Talpalar et al., 2013). The Shox2^{off} V2a commissural pathway seems to be active at medium to high speeds (Crone et al., 2009) and it is likely that non-V2a Shox2^{+} neurons, together with other yet-to-be-identified iEINs, drive left-right alternation at lower frequencies of locomotion. Therefore, left-right alternation at higher frequencies is supported by Shox2^{off} V2a INs and at lower speeds the other rhythm-generating iEINs are capable of maintaining left-right alternation (Figure 8B).

Transsynaptic virus injections demonstrate that many Shox2 INs are premotor INs and located in a lateral population within the spinal cord. Our findings that ablating Shox2^{+} V2a neurons in the Shox2-Chx10DTA mice does not affect the locomotor frequency but leads to increased variability of locomotor bursts strongly suggests that locomotor-related premotor Shox2 INs are Shox2^{+} V2a neurons. These Shox2^{+} V2a neurons would then be downstream of the rhythm-generating kernel (Figure 8B).

Flexor dominance was detected both in the firing of rhythmic Shox2 INs as well as connectivity profile analysis to motor neurons. In a comparative analysis, we detected approximately three times more Shox2 INs connecting to flexor (TA) than to extensor (GS) motor neurons. This observation is in line with previous findings showing that premotor neurons provide a much stronger synaptic excitation to flexor motor neurons than to extensor motor neurons during locomotor-like activity (Endo and Kiehn, 2008). Finally, premotor Shox2 INs were detected in a lateral position in the spinal cord, separated from Shox2 INs that are not connected to motor neurons. These findings support a view in which excitatory premotor neurons providing direct excitation to motor neurons are distinct from rhythm-generating excitatory neurons.

Molecularly Defined Neuronal Populations May Contribute to Multiple Network Functions

Shox2 INs are clearly not the only rhythm-generating neurons in the locomotor network since rhythm remains in the absence of the Shox2 INs, although reduced in frequency. The molecular identity of other contributing interneurons is not known. Moreover, even within the Shox2^{+} non-V2a neurons, rhythm generation may be distributed among neurons derived from several progenitor domains. The picture that emerges from our study is therefore that rhythm generation in the mammalian locomotor network seems to emerge from the combined action of multiple populations of molecularly defined neurons. Furthermore, our study shows that a single molecularly defined population may contribute to several aspects of the locomotor function. It is plausible that defining a finer-grained molecular code may help to clarify the identity of these functional subgroups.

EXPERIMENTAL PROCEDURES

All experimental procedures followed the guidelines of the Animal Welfare Agency and were approved by the local Animal Care and Use Committees and competent veterinary authorities.

Mice

For details of generation of the *Shox2::Cre* mouse line, see the Supplemental Experimental Procedures. The *chx10::LNL::DTA* mice were similar to those used in Crone et al. (2008). For conditional deletion of *vGluT2*, mice with loxP sites flanking exon 2 of the *Slc17a6* gene, which encodes for *vGluT2* were used (see Talpalar et al., 2011; Supplemental Experimental Procedures). *Rosa26-CAG-LSL-eNpHR3.0-EYFP-WPRE*, *ROSA26-YFP*, *Tau-GFP-nlsLacZ*, and the *Z/EG* mice were obtained from Jackson Laboratory.

Immunohistochemistry

Immunohistochemistry was performed using standard protocols with antibodies listed in the Supplemental Experimental Procedures.

In Situ Hybridization

Combined in situ hybridization histochemistry/immunohistochemistry was performed on 12–20 μm cryostat sections, omitting the proteinase K step. vGluT2 full-length (GenBank AI841371) and exon 2 riboprobes were used.

Evaluation of Midline Crossing

Midline crossing was evaluated by retrograde labeling with tetramethylrhodamine dextran (Supplemental Experimental Procedures).

Preparations for Electrophysiological Experiments

Spinal cords from mice aged 0–5 days (P0–5) were isolated. Transverse slice preparations were used for connectivity and morphology and rhythmicity studies while dorsal-horn-removed preparations (Dougherty and Kiehn, 2010a) were used for studies of rhythmicity (Supplemental Experimental Procedures). All preparations were perfused with Ringer's solution (111 NaCl, 3 KCl, 11 glucose, 25 $NaHCO_3$, 1.3 $MgSO_4$, 1.1 KH_2PO_4, 2.5 $CaCl_2$, pH 7.4, and aerated with 95% O_2/5% CO_2) at a flow rate of 4–5 ml/min. Ventral root activity (signal band-pass filtered 100–1,000 Hz; gain 5–10,000) was recorded from ventral roots in L1 L2, L3, L4, or L5 with glass suction electrodes.

Recordings from Shox2+ INs

Patch electrodes used for whole cell recordings of Shox2-GFP cells contained (in mM): 128 K-gluconate, 10 HEPES, 0.0001 $CaCl_2$, 1 glucose, 4 NaCl, 5 ATP, 0.3 GTP, at pH 7.4. Shox2-GFP cells were visually patched (Supplemental Experimental Procedures). Biocytin filled cells were after processing (Supplemental Experimental Procedures) traced postexperimentally using camera-lucida, scanned in, and retraced in CorelDraw.

Drugs

NMDA (5–10 μM) and 5-HT (8 μM) were bath-applied to induce locomotor-like activity.

Neural-Evoked Locomotor-like Activity

Brainstem-evoked locomotor-like activity was elicited as previously described (Talpalar et al., 2011).

Locomotor Analysis

The locomotor frequency (cycles per second, Hz) was calculated from 3–5 min of activity, taken at least 10 min after the initial burst of drug-induced activity, when the locomotor-like activity was stable. Locomotor-like activity was analyzed using rectified and smoothed (time constant of 0.2 s) signals of ventral root activity in either Spike2 (Cambridge Electronic Design) or a custom-made program in R package. Left-right and flexor-extensor coordination was assessed with circular statistic, where the vector direction gives the preferred phase of the activity and the length of the vector (r) the precision of the phase. p values larger than 0.05 determined by Rayleigh's test were considered nonsignificant. The degree of rhythmicity of individual Shox2-INs based firing or voltage fluctuations was also evaluated using circular statistics (Supplemental Experimental Procedures).

Viral Labeling of Premotor and Shox2 Neurons

Transsynaptic virus experiments using coinjection of attenuated rabies viruses and complementing AAV-G protein were carried out as previously described (Stepien et al., 2010; Tripodi et al., 2011; Supplemental Experimental Procedures). For intraspinal injections, floxed-AAV-Synaptophysin-GFP was injected intraspinally and unilaterally at P3, followed by targeted hindlimb muscle injections (TA and GS) of f-dextran at P8, and experiments were terminated at P17 for analysis.

Statistics

Values are reported as mean ± SEM. The level of significance was $p < 0.05$ for all statistical tests.

SUPPLEMENTAL INFORMATION

Supplemental Information includes Supplemental Experimental Procedures, three figures, and one table and can be found with this article online at http://dx.doi.org/10.1016/j.neuron.2013.08.015.

ACKNOWLEDGMENTS

This work was supported by the Swedish Research Council (to O.K.), ERC advanced grants (to O.K. and S.A.), the Torsten and Ragnar Söderberg Foundations (to O.K.), StratNeuro (to O.K.), a NINDS grant (to T.M.J.), ProjectALS (to T.M.J.), the HHMI (to T.M.J.), a Swiss National Science Foundation grant (to S.A. and D.S.), the Novartis Research Foundation (to S.A.), Kanton Basel-Stadt (to S.A.), National Science Foundation IRFP (to K.J.D.), the Helen Hay Whitney Foundation (to L.Z.), BRFAA (to L.Z.), and a Marie Curie Reintegration Grant (to L.Z.). We are grateful to Dr. Thomas Hnasko for providing the *vGluT2$^{lox/lox}$* mice, to Kamal Sharma for providing *Chx10lnlDTA* mice, and to Ann-Charlotte Westerdahl and Natalie Sleiers for technical assistance.

Accepted: August 9, 2013
Published: November 20, 2013

REFERENCES

Al-Mosawie, A., Wilson, J.M., and Brownstone, R.M. (2007). Heterogeneity of V2-derived interneurons in the adult mouse spinal cord. Eur. J. Neurosci. *26*, 3003–3015.

Buchanan, J.T., and Grillner, S. (1987). Newly identified 'glutamate interneurons' and their role in locomotion in the lamprey spinal cord. Science *236*, 312–314.

Bui, T.V., Akay, T., Loubani, O., Hnasko, T.S., Jessell, T.M., and Brownstone, R.M. (2013). Circuits for grasping: spinal dI3 interneurons mediate cutaneous control of motor behavior. Neuron *78*, 191–204.

Butt, S.J., and Kiehn, O. (2003). Functional identification of interneurons responsible for left-right coordination of hindlimbs in mammals. Neuron *38*, 953–963.

Butt, S.J., Lebret, J.M., and Kiehn, O. (2002a). Organization of left-right coordination in the mammalian locomotor network. Brain Res. Brain Res. Rev. *40*, 107–117.

Butt, S.J., Harris-Warrick, R.M., and Kiehn, O. (2002b). Firing properties of identified interneuron populations in the mammalian hindlimb central pattern generator. J. Neurosci. *22*, 9961–9971.

Cazalets, J.R. (2005). Metachronal propagation of motoneurone burst activation in isolated spinal cord of newborn rat. J. Physiol. *568*, 583–597.

Crone, S.A., Quinlan, K.A., Zagoraiou, L., Droho, S., Restrepo, C.E., Lundfald, L., Endo, T., Setlak, J., Jessell, T.M., Kiehn, O., and Sharma, K. (2008). Genetic ablation of V2a ipsilateral interneurons disrupts left-right locomotor coordination in mammalian spinal cord. Neuron *60*, 70–83.

Crone, S.A., Zhong, G., Harris-Warrick, R., and Sharma, K. (2009). In mice lacking V2a interneurons, gait depends on speed of locomotion. J. Neurosci. *29*, 7098–7109.

Dougherty, K.J., and Kiehn, O. (2010a). Firing and cellular properties of V2a interneurons in the rodent spinal cord. J. Neurosci. *30*, 24–37.

Dougherty, K.J., and Kiehn, O. (2010b). Functional organization of V2a-related locomotor circuits in the rodent spinal cord. Ann. N Y Acad. Sci. *1198*, 85–93.

Eklöf-Ljunggren, E., Haupt, S., Ausborn, J., Dehnisch, I., Uhlén, P., Higashijima, S., and El Manira, A. (2012). Origin of excitation underlying locomotion in the spinal circuit of zebrafish. Proc. Natl. Acad. Sci. USA *109*, 5511–5516.

Endo, T., and Kiehn, O. (2008). Asymmetric operation of the locomotor central pattern generator in the neonatal mouse spinal cord. J. Neurophysiol. *100*, 3043–3054.

Ericson, J., Rashbass, P., Schedl, A., Brenner-Morton, S., Kawakami, A., van Heyningen, V., Jessell, T.M., and Briscoe, J. (1997). Pax6 controls progenitor

cell identity and neuronal fate in response to graded Shh signaling. Cell *90*, 169–180.

Gosgnach, S., Lanuza, G.M., Butt, S.J., Saueressig, H., Zhang, Y., Velasquez, T., Riethmacher, D., Callaway, E.M., Kiehn, O., and Goulding, M. (2006). V1 spinal neurons regulate the speed of vertebrate locomotor outputs. Nature *440*, 215–219.

Goulding, M. (2009). Circuits controlling vertebrate locomotion: moving in a new direction. Nat. Rev. Neurosci. *10*, 507–518.

Grillner, S. (2003). The motor infrastructure: from ion channels to neuronal networks. Nat. Rev. Neurosci. *4*, 573–586.

Grillner, S. (2006). Biological pattern generation: the cellular and computational logic of networks in motion. Neuron *52*, 751–766.

Grillner, S., and Jessell, T.M. (2009). Measured motion: searching for simplicity in spinal locomotor networks. Curr. Opin. Neurobiol. *19*, 572–586.

Helms, A.W., and Johnson, J.E. (2003). Specification of dorsal spinal cord interneurons. Curr. Opin. Neurobiol. *13*, 42–49.

Hinckley, C.A., and Ziskind-Conhaim, L. (2006). Electrical coupling between locomotor-related excitatory interneurons in the mammalian spinal cord. J. Neurosci. *26*, 8477–8483.

Jankowska, E. (2008). Spinal interneuronal networks in the cat: elementary components. Brain Res. Rev. *57*, 46–55.

Jessell, T.M. (2000). Neuronal specification in the spinal cord: inductive signals and transcriptional codes. Nat. Rev. Genet. *1*, 20–29.

Jonas, P., Bischofberger, J., and Sandkühler, J. (1998). Corelease of two fast neurotransmitters at a central synapse. Science *281*, 419–424.

Kiehn, O. (2006). Locomotor circuits in the mammalian spinal cord. Annu. Rev. Neurosci. *29*, 279–306.

Kiehn, O., and Kjaerulff, O. (1998). Distribution of central pattern generators for rhythmic motor outputs in the spinal cord of limbed vertebrates. Ann. N Y Acad. Sci. *860*, 110–129.

Li, W.C., Soffe, S.R., Wolf, E., and Roberts, A. (2006). Persistent responses to brief stimuli: feedback excitation among brainstem neurons. J. Neurosci. *26*, 4026–4035.

Lundfald, L., Restrepo, C.E., Butt, S.J., Peng, C.Y., Droho, S., Endo, T., Zeilhofer, H.U., Sharma, K., and Kiehn, O. (2007). Phenotype of V2-derived interneurons and their relationship to the axon guidance molecule EphA4 in the developing mouse spinal cord. Eur. J. Neurosci. *26*, 2989–3002.

Madisen, L., Mao, T., Koch, H., Zhuo, J.M., Berenyi, A., Fujisawa, S., Hsu, Y.W., Garcia, A.J., 3rd, Gu, X., Zanella, S., et al. (2012). A toolbox of Cre-dependent optogenetic transgenic mice for light-induced activation and silencing. Nat. Neurosci. *15*, 793–802.

McLean, D.L., Masino, M.A., Koh, I.Y., Lindquist, W.B., and Fetcho, J.R. (2008). Continuous shifts in the active set of spinal interneurons during changes in locomotor speed. Nat. Neurosci. *11*, 1419–1429.

Müller, T., Brohmann, H., Pierani, A., Heppenstall, P.A., Lewin, G.R., Jessell, T.M., and Birchmeier, C. (2002). The homeodomain factor lbx1 distinguishes two major programs of neuronal differentiation in the dorsal spinal cord. Neuron *34*, 551–562.

Panayi, H., Panayiotou, E., Orford, M., Genethliou, N., Mean, R., Lapathitis, G., Li, S., Xiang, M., Kessaris, N., Richardson, W.D., and Malas, S. (2010). Sox1 is required for the specification of a novel p2-derived interneuron subtype in the mouse ventral spinal cord. J. Neurosci. *30*, 12274–12280.

Parker, D., and Grillner, S. (2000). The activity-dependent plasticity of segmental and intersegmental synaptic connections in the lamprey spinal cord. Eur. J. Neurosci. *12*, 2135–2146.

Peng, C.Y., Yajima, H., Burns, C.E., Zon, L.I., Sisodia, S.S., Pfaff, S.L., and Sharma, K. (2007). Notch and MAML signaling drives Scl-dependent interneuron diversity in the spinal cord. Neuron *53*, 813–827.

Quinlan, K.A., and Kiehn, O. (2007). Segmental, synaptic actions of commissural interneurons in the mouse spinal cord. J. Neurosci. *27*, 6521–6530.

Roberts, A., Soffe, S.R., Wolf, E.S., Yoshida, M., and Zhao, F.Y. (1998). Central circuits controlling locomotion in young frog tadpoles. Ann. N Y Acad. Sci. *860*, 19–34.

Stepien, A.E., Tripodi, M., and Arber, S. (2010). Monosynaptic rabies virus reveals premotor network organization and synaptic specificity of cholinergic partition cells. Neuron *68*, 456–472.

Talpalar, A.E., Endo, T., Löw, P., Borgius, L., Hägglund, M., Dougherty, K.J., Ryge, J., Hnasko, T.S., and Kiehn, O. (2011). Identification of minimal neuronal networks involved in flexor-extensor alternation in the mammalian spinal cord. Neuron *71*, 1071–1084.

Talpalar, A.E., Bouvier, J., Borgius, L., Fortin, G., Pierani, A., and Kiehn, O. (2013). Dual-mode operation of neuronal networks involved in left-right alternation. Nature *500*, 85–88.

Tripodi, M., Stepien, A.E., and Arber, S. (2011). Motor antagonism exposed by spatial segregation and timing of neurogenesis. Nature *479*, 61–66.

Warp, E., Agarwal, G., Wyart, C., Friedmann, D., Oldfield, C.S., Conner, A., Del Bene, F., Arrenberg, A.B., Baier, H., and Isacoff, E.Y. (2012). Emergence of patterned activity in the developing zebrafish spinal cord. Curr. Biol. *22*, 93–102.

Wilson, J.M., Hartley, R., Maxwell, D.J., Todd, A.J., Lieberam, I., Kaltschmidt, J.A., Yoshida, Y., Jessell, T.M., and Brownstone, R.M. (2005). Conditional rhythmicity of ventral spinal interneurons defined by expression of the Hb9 homeodomain protein. J. Neurosci. *25*, 5710–5719.

Zagoraiou, L., Akay, T., Martin, J.F., Brownstone, R.M., Jessell, T.M., and Miles, G.B. (2009). A cluster of cholinergic premotor interneurons modulates mouse locomotor activity. Neuron *64*, 645–662.

Zhong, G., Díaz-Ríos, M., and Harris-Warrick, R.M. (2006). Intrinsic and functional differences among commissural interneurons during fictive locomotion and serotonergic modulation in the neonatal mouse. J. Neurosci. *26*, 6509–6517.

Zhong, G., Droho, S., Crone, S.A., Dietz, S., Kwan, A.C., Webb, W.W., Sharma, K., and Harris-Warrick, R.M. (2010). Electrophysiological characterization of V2a interneurons and their locomotor-related activity in the neonatal mouse spinal cord. J. Neurosci. *30*, 170–182.